

# Biobased Nanoparticles for Broadband UV Protection with Photostabilized UV Filters

Douglas R. Hayden,<sup>\*,†</sup> Arnout Imhof,<sup>\*,†</sup> and Krassimir P. Velikov<sup>†,‡</sup>

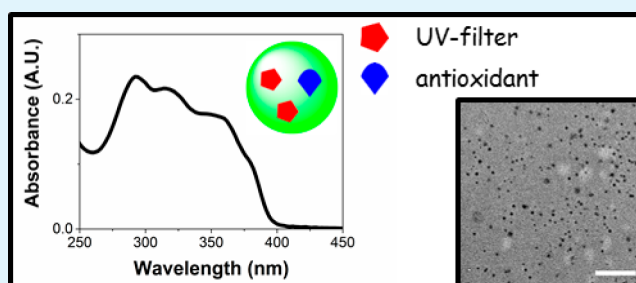
<sup>†</sup>Soft Condensed Matter, Debye Institute for Nanomaterials Science, Utrecht University, Princetonplein 1, 3584 CC Utrecht, The Netherlands

<sup>‡</sup>Unilever R&D Vlaardingen, Olivier van Noortlaan 120, 3133 AT Vlaardingen, The Netherlands

## S Supporting Information

**ABSTRACT:** Sunscreens rely on multiple compounds to provide effective and safe protection against UV radiation. UV filters in sunscreens, in particular, provide broadband UV protection but are heavily linked to adverse health effects due to the generation of carcinogenic skin-damaging reactive oxygen species (ROS) upon solar irradiation. Herein, we demonstrate significant reduction in the ROS concentration by encapsulating an antioxidant photostabilizer with multiple UV filters into biobased ethyl cellulose nanoparticles. The developed nanoparticles display complete broadband UV protection and can form transparent and flexible films. This system therefore shows significant potential toward effective and safe nanoparticle-based UV protective coatings.

**KEYWORDS:** sunscreens, UV filters, antioxidants, reactive oxygen species, ethyl cellulose



An essential issue within consumer products is protection against ultraviolet (UV) radiation. UV protection within food and packaging materials is required for retarding chemical degradation, whereas UV protection within personal care products (i.e., sunscreens) is imperative for the preservation of human health as excessive exposure to UV-radiation accounts for the vast majority of skin cancers.<sup>1–3</sup> The main requirements and challenges in the preparation of UV-protective coatings are (i) to provide broad protection over the entire UVA/UVB spectrum, and (ii) to maintain photostability after extended periods of irradiation.<sup>4–6</sup> Currently, broad UV spectrum protection is realized via the use of multiple organic UV filters (e.g., avobenzene, octinoxate, oxybenzone, padimate-O, octocrylene) together in sunscreen formulations where the UV filters are solubilized via emulsions. There is, however, considerable concern regarding the production of carcinogenic reactive oxygen species (ROS) by organic UV filters because of photodegradation when exposed to sunlight.<sup>7,8</sup> To address the issue, antioxidants (i.e.,  $\alpha$ -tocopherol) are added to sunscreen formulations in order to scavenge generated ROS, thus providing photostabilization.<sup>9–11</sup> Minimising skin contact with UV filters is also desirable due to concern over adverse effects caused by systemic absorption of UV filters penetrating the skin.<sup>12,13</sup> This has led to interest involving encapsulation into nanoparticles to reduce their (photo)-toxicity.<sup>14–17</sup> Encapsulation into nanoparticles provides further advantages such as the amount of UV filter added to a formulation is no longer limited by its solubility in the solvent/vehicle,<sup>18</sup> photodegradation can be stymied,<sup>15</sup> and the need for unnecessary chemicals (i.e., surfactants, organic

solvents) is reduced. So far, encapsulation has been most popular using materials such as solid–lipid nanoparticles (SLNs),<sup>19</sup> poly(D,L-lactide) particles,<sup>12,15</sup> and silica.<sup>14,16,20,21</sup> Notably, SLNs have shown to be suitable carriers for encapsulating UV filter “couples”, two UV filters into the same carrier, in order to provide broader UV spectrum protection.<sup>22</sup> Nanoparticle-based UV-protective coatings still, however, need to meet the requirements currently faced by sunscreens. Therefore, there is a need to develop nanoparticles which can effectively encapsulate multiple UV filters and antioxidants all together, regardless of their initial physical states (liquid/solid), in order to provide broadband UV spectrum protection and vital photostabilization concerning protection against ROS. Furthermore, the developed nanoparticles should be biobased for maximum cosmetic appeal and also suitable for multiple solvent systems. Nanoparticles that can be dispersed in multiple solvent systems offer versatility for usage within many different sunscreen formulation types (e.g., oil, emulsion). SLNs for instance, although biobased, are not suitable for oil-based formulations as they will simply dissolve. Herein, we therefore demonstrate the encapsulation of multiple UV filters together with an antioxidant into biobased and environmentally benign nanoparticles designed from ethyl cellulose (EC). EC is a material with potential for use within many solvent systems. We show that broadband UV spectrum protection can be achieved and that the concentration of ROS

Received: October 11, 2016

Accepted: November 22, 2016

Published: November 22, 2016



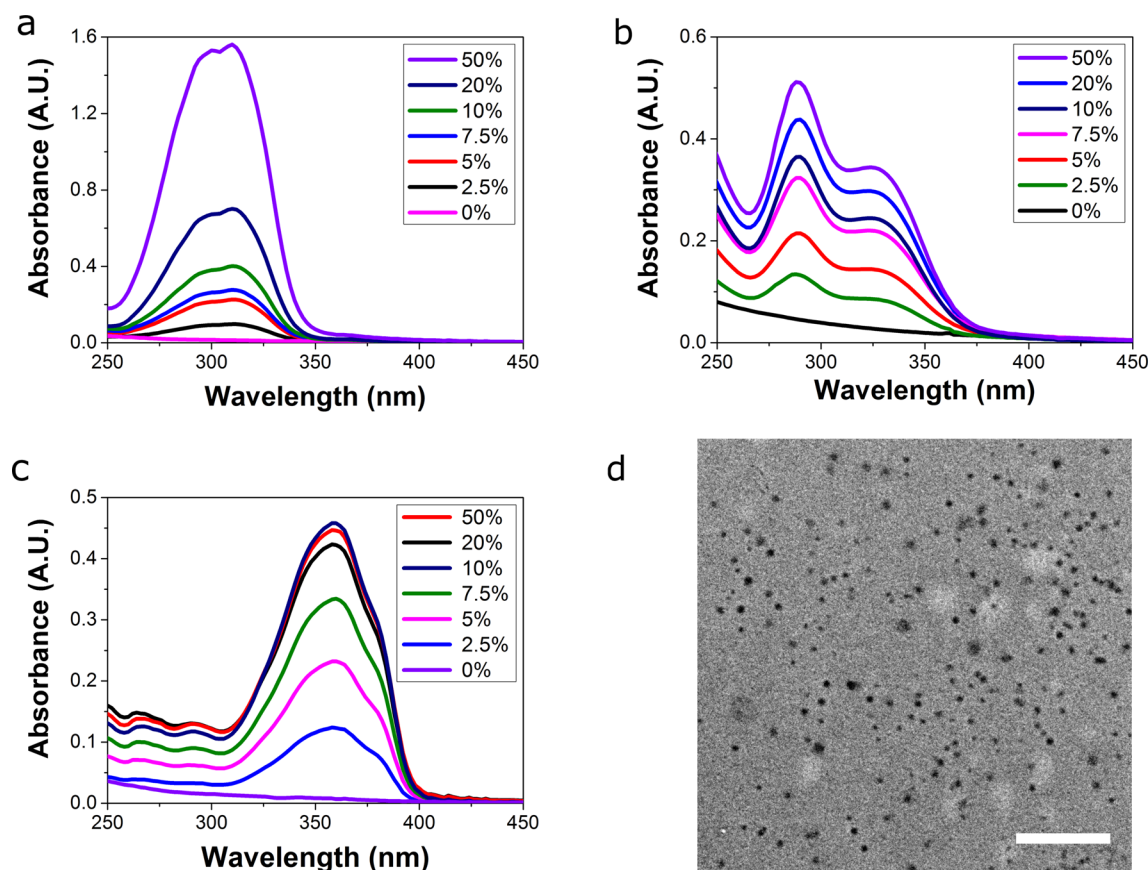


**Figure 1.** (a–c) Absorption spectra for a series of ECNPs prepared in which varying amounts of UV filter (a) octinoxate, (b) oxybenzone, and (c) avobenzone have been added to the synthesis. The concentration of all aqueous ECNPs dispersions measured here are equal ( $5.35 \times 10^{-3} \text{ g L}^{-1}$ ). “50%” is a weight percentage indicating, for example, 0.5 g of UV filter was added to 1 g of EC. (d) TEM image of ECNPs with encapsulated octinoxate. Scale bar 500 nm.

within the ethyl cellulose nanoparticles (ECNPs) is reduced upon the encapsulation of an antioxidant. Furthermore, considering the application of UV-protective coatings we show the ability to form uniform, transparent, flexible, UV protective coatings from the ECNPs.

ECNPs, with a desirable size for cosmetic applications (<100 nm) were prepared using a modified “anti-solvent precipitation” procedure of that from literature.<sup>23</sup> This was chosen primarily for its up-scalable potential. Here, ethyl cellulose was dissolved in ethanol before being poured into a large volume of water resulting in spontaneous formation of ECNPs. Removal of the ethanol (and some water) by rotary evaporation resulted in a stable aqueous dispersion of ECNPs with an average size of 50 nm and narrow distribution (Figure S1). We then investigated the encapsulation of three commonplace UV filters separately, which together span the entire UVA/UVB spectrum (oxybenzone, avobenzone, and octinoxate), into ECNPs. The encapsulation procedure relies on the coprecipitation of the hydrophobic UV filters together with the EC. To physically encapsulate UV filters into ECNPs, the individual UV filter was dissolved with the ethyl cellulose in ethanol before undergoing the antisolvent precipitation to form ECNPs with encapsulated UV filter. For each of the three model UV filters the encapsulation efficiency and the maximum amount of UV filter encapsulated into ECNPs were explored. To explore this, we prepared a series of dispersions for each UV filter in which increasing amounts of the UV filter were added to the synthesis along with the EC. To clarify, the amount of EC used

in the synthesis was always kept constant but the amount of UV filter was varied. Figure 1 shows three absorption spectra, one for each UV filter series, for the resulting aqueous dispersions of ECNPs. The spectra clearly show the efficient encapsulation of all UV filters tested. There is a general trend that the more UV filter initially added to the synthesis the more encapsulated, which is intuitive. However, in the two series involving encapsulating avobenzone and oxybenzone the maximum absorbance appears to level off for the addition of greater amounts of UV filter. This leveling off indicates that the ECNPs become completely saturated with UV filter to a point in which they cannot encapsulate any greater amounts. This result is consistent with the experimental observation that increasing amounts of nondispersed aggregates were seen. Transmission electron microscopy (TEM) imaging (Figure 1d) and dynamic light scattering (DLS) measurements (Figure S1) indicated no change in morphology/size of the nanoparticles upon encapsulation of the UV filters.

To provide full UV spectrum coverage with the ECNPs, we prepared ECNPs with multiple UV filters encapsulated together. To achieve this, the same antisolvent precipitation technique used before to encapsulate an individual UV filter was implemented. Thus, equal amounts (by weight) of the three UV filters (oxybenzone, avobenzone, octinoxate) were dissolved with EC in ethanol before pouring into water. After evaporation of the ethanol, an aqueous dispersion of ECNPs with multiple UV filters encapsulated was prepared. From the spectra in Figure 2a, b, it is clear that by encapsulating all three

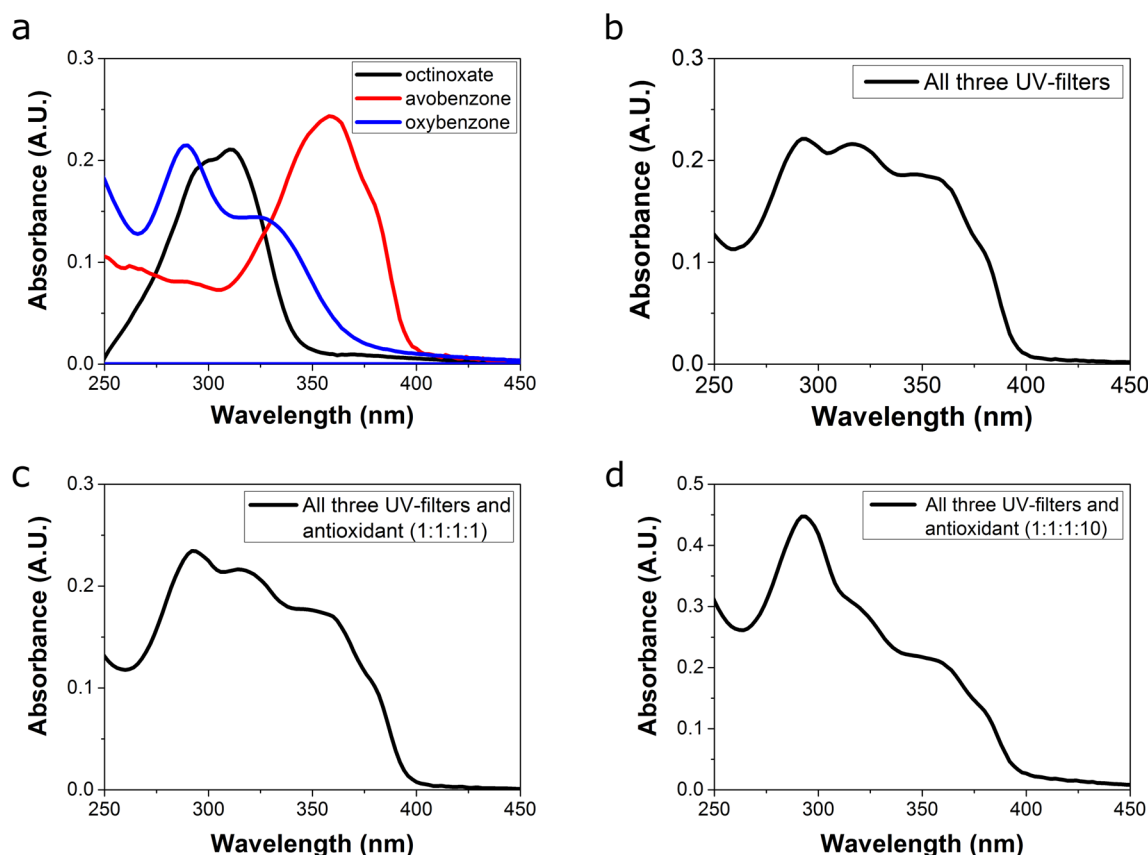


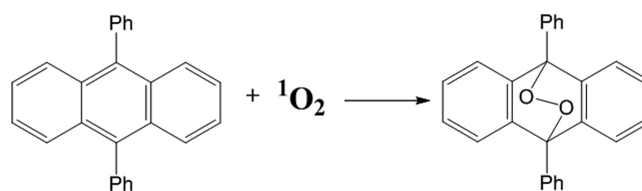
**Figure 2.** (a, b) Absorption spectra of ECNPs with equivalent amounts (by weight) of encapsulated UV filters octinoxate, oxybenzone, and avobenzone, (a) individually and (b) together. (c, d) Absorption spectra of ECNPs containing these three UV filters and an antioxidant ( $\alpha$ -tocopherol ( $\lambda = 288$  nm)) all encapsulated together, (c) in equivalent amounts (by weight) and (d) with more  $\alpha$ -tocopherol relative to the UV filters (mass ratio 1:1:1:10). Increasing the mass ratio as in (d) accentuates the presence of the  $\alpha$ -tocopherol.

UV filters together the ECNPs provide protection across the entire UVA/UVB spectrum ( $\lambda = 290$ – $380$  nm).

To address the issue of large concentrations of ROS generated by UV filters when irradiated by sunlight, we encapsulated an antioxidant along with the UV filters. We chose  $\alpha$ -tocopherol as the model antioxidant to be encapsulated as a result of the many independent studies demonstrating the photostabilizing effect when used in combination with UV filters.<sup>9,10,24</sup>  $\alpha$ -tocopherol has an absorption maximum at  $\lambda = 288$  nm, which overlaps with that of octinoxate and oxybenzone but is far less prominent. Despite this, however, its presence can be seen by these absorption spectra since there is a slight absorbance increase at  $\lambda = 288$  nm (Figure 2c), which becomes more prominent upon the addition of more  $\alpha$ -tocopherol (Figure 2d). We found these ECNPs with encapsulated UV filters and antioxidant maintained a high level of stability with respect to the loss of absorbance as a function of time when irradiated by artificial sunlight (Figure S2).

We devised an experiment to test whether the encapsulated antioxidant reduced the concentration of carcinogenic ROS within the ECNPs by using the ROS scavenger 9,10-diphenylanthracene (DPA). DPA is well-known as a ROS—in particular, singlet oxygen species ( $^1\text{O}_2$ )—scavenger, used for the quantification of  $^1\text{O}_2$ .<sup>25</sup> DPA absorbs UV light whereas its reaction product with  $^1\text{O}_2$  (DPA-endoperoxide) does not (Scheme 1), so monitoring the degradation of the absorbance of DPA at  $\lambda_{\text{max}} = 376$  nm indirectly provides an indication of the amount of  $^1\text{O}_2$  species produced.

#### Scheme 1. Reaction of Diphenylanthracene (DPA) with a Singlet Oxygen Species To Form DPA-Endoperoxide



An aqueous dispersion of ECNPs with encapsulated DPA was irradiated by artificial sunlight. DPA was found to degrade significantly under UV-light itself. We found that encapsulating the UV filter octinoxate—known to produce  $^1\text{O}_2$ <sup>26</sup>—along with DPA did result in even greater degradation, although this was a relatively small increase. We demonstrated that the encapsulation of the antioxidant significantly suppresses this degradation (Figure 3a, b), and that a greater amount of encapsulated antioxidant results in slightly greater suppression (Figure 3c). Therefore, we demonstrated that the encapsulation of an antioxidant reduces the concentration of carcinogenic  $^1\text{O}_2$  within the ECNPs.

Finally, transparent, flexible and uniform UV-protective coatings were prepared by spin coating a concentrated dispersion ( $290 \text{ g L}^{-1}$ ) of the ECNPs containing encapsulated UV filters avobenzone, oxybenzone, and octinoxate in equal amounts onto plasma-cleaned glass microscope coverslips at 1500 rpm for 1 min (Figure 4a). We found that coating subsequent layers upon the original layer—a well-established

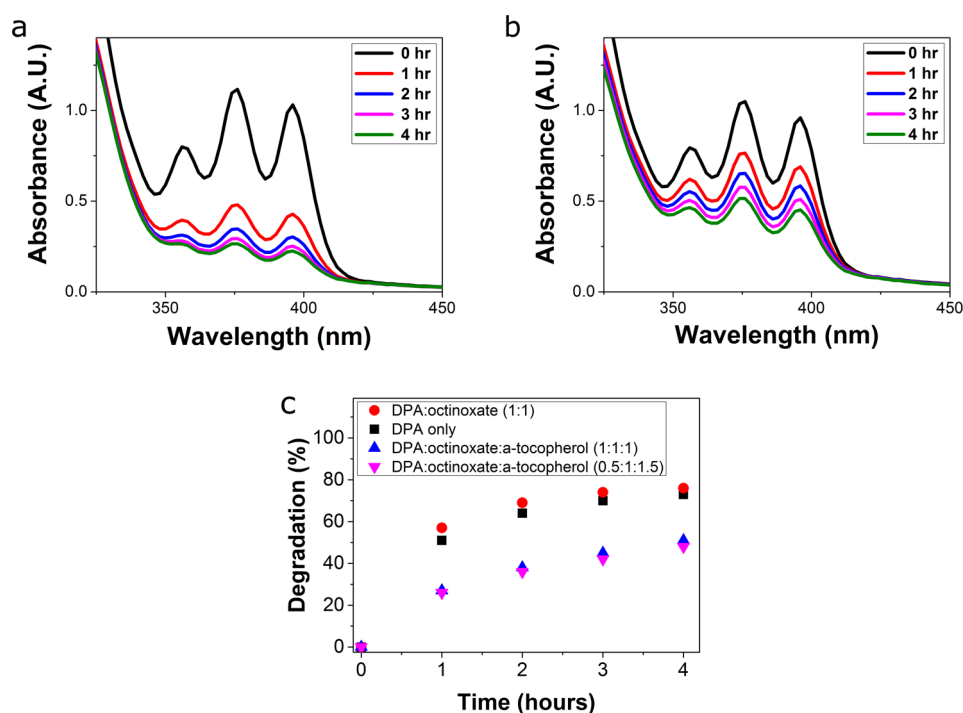


**Figure 3.** (a, b) Absorption spectra showing the degradation of the absorbance of singlet oxygen ( $^1\text{O}_2$ ) scavenger DPA encapsulated into ECNPs as a function of time when irradiated by artificial sunlight. DPA itself degrades under UV-irradiation to a certain extent but also due to the reaction with  $^1\text{O}_2$  to form DPA-endoperoxide (Scheme 1), which unlike DPA does not absorb in the 500–300 nm range. The decrease in absorbance at  $\lambda = 376$  nm therefore is an indication for the amount of  $^1\text{O}_2$  in the ECNPs. (a) ECNPs contain DPA and octinoxate only (mass ratio 1:1) and significant degradation at  $\lambda = 376$  nm is observed. (b) ECNPs contain DPA, octinoxate, and  $\alpha$ -tocopherol (mass ratio 1:1:1) and this degradation at  $\lambda = 376$  nm is considerably suppressed as a result of the  $\alpha$ -tocopherol presence reducing the concentration of  $^1\text{O}_2$ . (c) displays these degradations from a and b as a percentage as a function of time, as well as cases not shown in which the degradation was monitored for (i) ECNPs with DPA only and (ii) ECNPs with DPA, octinoxate, and  $\alpha$ -tocopherol but with a greater amount of  $\alpha$ -tocopherol than in b.

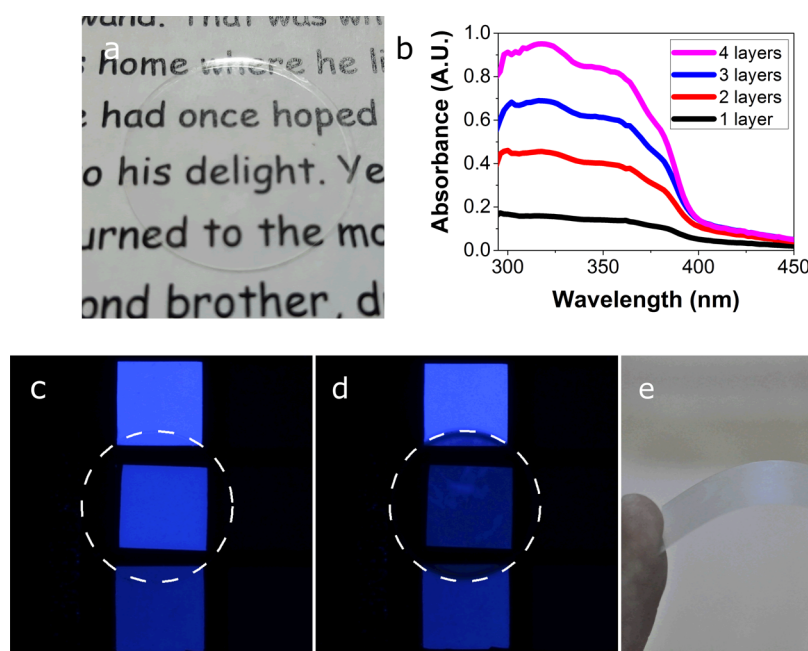


**Figure 4.** (a) Photo of a coated glass coverslip with a transparent, uniform, UV-protective coating. (b) Absorption spectrum showing the absorbance exhibited when multiple layers are spin coated. Wavelengths lower than  $\lambda = 290$  nm are not shown as they are absorbed by the glass coverslip. (c, d) Three UV-induced (by a  $\lambda = 375$  nm LED) fluorescent squares in which the middle square has either: (c) a plain glass coverslip or (d) our multiple-coated glass coverslip on top of it. The middle square with the UV-protective coated glass slide (border indicated by the dashed line) appears considerably darker than that of the plain glass slide because the coating - containing encapsulated UV filters in the ECNPs - blocks UV-light from passing through it and stimulating the square to fluoresce. The top and bottom squares are references. (e) Photo of a coated rectangular glass coverslip with an intact coating upon bending, showing that the coating is flexible.



technique in spin coating—allowed complete flexibility to tune the coating UV protection that we desired (Figure 4b). We observed that the coating remained transparent to visible light when the glass was coated with multiple layers, but was effective in blocking out UV light (Figure 4c, d). Furthermore, the coating is completely flexible (Figure 4e) in contrast with sol-gel inorganic coatings,<sup>21</sup> rendering it attractive for applications in, for example, UV-protective food packaging materials. By SEM (scanning electron microscopy) imaging we observed that a three layer coating was  $235 \pm 18$  nm thick (Figure S3); therefore, we deduced that each coating layer was  $78 \pm 6$  nm thick, assuming each layer contributes an equal amount to the overall coating. Thus, to get a coating that filters 90% of UVA-light (sun protection factor (SPF) = 10) at, for example,  $\lambda = 320$  nm (absorbance = 0.68 A.U. for three-layer coating), a coating thickness of 391 nm is required.

In conclusion, the encapsulation of multiple UV filters along with a photostabilizing antioxidant into nanoparticles designed from ethyl cellulose (ECNPs) was demonstrated. Importantly, the addition of this antioxidant photostabilizer ( $\alpha$ -tocopherol) showed significant reduction of the concentration of carcinogenic ROS within the ECNPs, known to be produced by UV filters. These nanoparticle carriers effectively encapsulated all the UV filters (oxybenzone, avobenzone, octinoxate) and the antioxidant tested resulting in ECNPs with complete UVA/UVB protection and photostabilized UV filters. Moreover, considering that these nanoparticles are interesting for the application of UV-protective coatings, the ability for these nanoparticles to form transparent, uniform, flexible, UV-protective coatings with tunable thicknesses and SPF were also demonstrated. As interest for nanoparticle use within sunscreens grows because of the substantial concerns associated with UV filter-skin contact, it must be demonstrated that suitable options exist that fulfill the requirements. Here, we present a step toward realizing this goal.

## ■ ASSOCIATED CONTENT

### Supporting Information

The Supporting Information is available free of charge on the ACS Publications website at DOI: 10.1021/acsami.6b12933.

Experimental, materials and methods, DLS and TEM/cryo-TEM images of ECNPs, photostability measurements of ECNPs with encapsulated UV filters and antioxidant, analysis of coating thickness with SEM imaging (PDF)

## ■ AUTHOR INFORMATION

### Corresponding Authors

\*E-mail: d.r.hayden@uu.nl.

\*E-mail: a.imhof@uu.nl.

### ORCID

Douglas R. Hayden: 0000-0001-7380-6054

Arnout Imhof: 0000-0002-7445-1360

Krassimir P. Velikov: 0000-0002-8838-1201

### Notes

The authors declare no competing financial interest.

## ■ ACKNOWLEDGMENTS

This research is supported by the Dutch Technology Foundation STW (Grant 13567), which is part of The Netherlands Organization for Scientific Research (NWO) and

partly funded by the Ministry of Economic Affairs. We thank Chris Schneidenburg and Dave van den Heuvel for technical assistance. We also thank Wiebke Albrecht and Tonnishtha Dasgupta for careful reading of the manuscript.

## ■ ABBREVIATIONS

UV, ultraviolet  
ECNPs, ethyl cellulose nanoparticles  
DPA, diphenylanthracene  
ROS, reactive oxygen species  
DLS, dynamic light scattering  
SEM, scanning electron microscopy

## ■ REFERENCES

- (1) Corbyn, Z. Lessons from a Sunburnt Country. *Nature* **2014**, *515*, S114.
- (2) Stavros, V. G. Photochemistry: A Bright Future for Sunscreens. *Nat. Chem.* **2014**, *6*, 955–956.
- (3) Viro, A.; Sanchez-Laorden, B.; Pedersen, M.; Furney, S. J.; Rae, J.; Hogan, K.; Ejima, S.; Girotti, M. R.; Cook, M.; Dhomen, N.; Marais, R. Ultraviolet Radiation Accelerates BRAF-Driven Melanoma-gensis by Targeting TP53. *Nature* **2014**, *511*, 478–482.
- (4) Morabito, K.; Shapley, N. C.; Steeley, K. G.; Tripathi, A. Review of Sunscreen and the Emergence of Non-Conventional Absorbers and Their Applications in Ultraviolet Protection. *Int. J. Cosmet. Sci.* **2011**, *33*, 385–390.
- (5) Bens, G. Sunscreens. In *Sunlight, Vitamin D and Skin Cancer*, 2nd ed.; Reichrath, J., Ed.; Advances in Experimental Medicine and Biology Series; Landes Bioscience and Springer Science + Business: Austin, TX, and New York, 2014; Vol 810, Chapter 25, pp 429–463.
- (6) Mancebo, S. E.; Hu, J. Y.; Wang, S. Q. Sunscreens: A Review of Health Benefits, Regulations, and Controversies. *Dermatol. Clin.* **2014**, *32*, 427–438.
- (7) Biba, E. The Sunscreen Pill. *Nature* **2014**, *515*, S124–125.
- (8) Damiani, E.; Baschong, W.; Greci, L. UV-Filter Combinations under UV-A Exposure: Concomitant Quantification of overall Spectral Stability and Molecular Integrity. *J. Photochem. Photobiol., B* **2007**, *87*, 95–104.
- (9) Oresajo, C.; Yatskayer, M.; Galdi, A.; Foltis, P.; Pillai, S. Complementary Effects of Antioxidants and Sunscreens in Reducing UV-Induced Skin Damage as Demonstrated by Skin Biomarker Expression. *J. Cosmet. Laser Ther.* **2010**, *12*, 157–162.
- (10) Kockler, J.; Oelgemöller, M.; Robertson, S.; Glass, B. D. Photostability of Sunscreens. *J. Photochem. Photobiol., C* **2012**, *13*, 91–110.
- (11) González, S.; Fernández-Lorente, M.; Gilaberte-Calzada, Y. The Latest on Skin Photoprotection. *Clin. Dermatol.* **2008**, *26*, 614–626.
- (12) Deng, Y.; Ediriwickrema, A.; Yang, F.; Lewis, J.; Girardi, M.; Saltzman, W. M. A Sunblock Based on Bioadhesive Nanoparticles. *Nat. Mater.* **2015**, *14*, 1278–1285.
- (13) Janjua, N. R.; Mogensen, B.; Andersson, A. M.; Petersen, J. H.; Henriksen, M.; Skakkebæk, N. E.; Wulf, H. C. Systemic Absorption of the Sunscreens Benzophenone-3, Octyl- Methoxycinnamate, and 3-(4-Methyl-Benzylidene) Camphor after Whole-Body Topical Application and Reproductive Hormone Levels in Humans. *J. Invest. Dermatol.* **2004**, *123*, 57–61.
- (14) Tolbert, S. H.; McFadden, P. D.; Loy, D. A. New Hybrid Organic/Inorganic Polysilsesquioxane-Silica Particles as Sunscreens. *ACS Appl. Mater. Interfaces* **2016**, *8*, 3160–3174.
- (15) Perugini, P.; Simeoni, S.; Scalia, S.; Genta, I.; Modena, T.; Conti, B.; Pavanetto, F. Effect of Nanoparticle Encapsulation on the Photostability of the Sunscreen Agent, 2-Ethylhexyl-P-Methoxycinnamate. *Int. J. Pharm.* **2002**, *246*, 37–45.
- (16) Lapidot, N.; Gans, O.; Biagini, F.; Sosonkin, L.; Rottman, C. Advanced Sunscreens: UV Absorbers Encapsulated in Sol-Gel Glass Microcapsules. *J. Sol-Gel Sci. Technol.* **2003**, *26*, 67–72.

- (17) Jiménez, M. M.; Pelletier, J.; Bobin, M. F.; Martini, M. C. Influence of Encapsulation on the in Vitro Percutaneous Absorption of Octyl Methoxycinnamate. *Int. J. Pharm.* **2004**, *272*, 45–55.
- (18) Herzog, B.; Hüglin, D.; Borsos, E.; Stehlin, A.; Luther, H. New UV Absorbers for Cosmetic Sunscreens - A Breakthrough for the Photoprotection of Human Skin. *Chimia* **2004**, *58*, 554–559.
- (19) Wissing, S. A.; Muller, R. H. Solid Lipid Nanoparticles as Carrier for Sunscreens: In Vitro Release and in Vivo Skin Penetration. *J. Controlled Release* **2002**, *81*, 225–233.
- (20) Kim, S. S.; Kim, V.; Kim, Y. B. Preparation and Characterization of Polysilsesquioxane Particles Containing UV-Absorbing Groups. *Macromol. Res.* **2012**, *20*, 437–446.
- (21) Cui, H.; Zayat, M.; Parejo, P. G.; Levy, D. Highly Efficient Inorganic Transparent UV-Protective Thin-Film Coating by Low Temperature Sol-Gel Procedure for Application on Heat-Sensitive Substrates. *Adv. Mater.* **2008**, *20*, 65–68.
- (22) Niculae, G.; Badea, N.; Meghea, A.; Oprea, O.; Lacatusu, I. Coencapsulation of Butyl-Methoxydibenzoylmethane and Octocrylene into Lipid Nanocarriers: UV Performance, Photostability and in Vitro Release. *Photochem. Photobiol.* **2013**, *89*, 1085–1094.
- (23) Bizmark, N.; Ioannidis, M. A.; Henneke, D. E. Irreversible Adsorption-Driven Assembly of Nanoparticles at Fluid Interfaces Revealed by a Dynamic Surface Tension Probe. *Langmuir* **2014**, *30*, 710–717.
- (24) Manesh, K. M.; Cardona, M.; Yuan, R.; Clark, M.; Kagan, D.; Balasubramanian, S.; Wang, J. Template-Assisted Fabrication of Salt-Independent Catalytic Tubular Microengines. *ACS Nano* **2010**, *4*, 1799–1804.
- (25) Steinbeck, M. J.; Khan, A. U.; Karnovsky, M. J. Extracellular Production of Singlet Oxygen by Stimulated Macrophages Quantified Using 9,10-Diphenylanthracene and Perylene in a Polystyrene Film. *J. Biol. Chem.* **1993**, *268*, 15649–15654.
- (26) Allen, J. M.; Gossett, C. J.; Allen, S. K. Photochemical Formation of Singlet Molecular Oxygen ( $^1O_2$ ) in Illuminated Aqueous Solutions of P-Aminobenzoic Acid (PABA). *J. Photochem. Photobiol., B* **1996**, *32*, 33–37.